2004 International Symposium on Nonlinear
Theory and its Applications (NOLTA2004)
Fukuoka, Japan, Nov. 29 - Dec. 3, 2004

Analysis of Piecewise Constant Models of Power Converters

Takahiro Kabe†, Toshimichi Saito† and Hiroyuki Torikai†

†EECE Dept, Hosei University, Kajino-cho, Koganei, Tokyo, 184-8584 Japan
Email: { kabe@nonlinear, tsaito@, torikai@ } k.hosei.ac.jp

Abstract—This paper studies piecewise constant model of basic DC/DC converters: an extremely simple switched dynamical system having rich nonlinear phenomena. The model is transformed into a dimensionless equation characterized by two parameters and a piecewise linear 1D return map is derived. We then give the parameters conditions for basic chaotic and periodic phenomena and investigate rich super-stable periodic phenomena in the discontinuous conduction mode. We also discuss an application to interleaved buck converters with fast transient process.

1. Introduction

In variety of power electronics circuits nonlinear switching plays important role not only to realize desired operation but also to generate rich nonlinear phenomena [1]. DC/DC converters are typical power electronics circuits and the dynamics can be described by piecewise linear equation connected by the nonlinear switching: a kind of switched dynamical system. For the converters there exist interesting results for chaos and bifurcation phenomena [2]-[6]. Analysis of the phenomena is interesting basic problem and may contribute to improve the circuits performance [7] [8], however, the analysis is hard because of complex dynamics and large number of parameters.

This paper studies piecewise constant (ab. PWC) model of basic DC/DC converters. The PWC model can be derived by replacing the output load with a DC source provided the time constant is larger enough than the clock period [9] - [11]. This model has piecewise constant vector field, piecewise linear solution and piecewise linear the return map. These properties are well suited for theoretical analysis. In Refs. [9] and [10] such PWC models are used effectively to analyze bifurcation and spectrum property. In this paper the PWC model is transformed into a dimensionless equation where the original parameters are integrated into two essential parameters. We then derive 1D return map and clarify the parameters condition for generation of basic chaotic and periodic phenomena. Especially, we analyze some of complicated super-stable periodic phenomena in the discontinuous conduction mode (ab. DCM). Such phenomena in DCM have not been discussed sufficiently so far in the existing literatures. Experimental confirmation of typical phenomena can be fund in [12]. We also discuss an application to interleaved buck converters having fast transient process and effective current sharing for lower voltages with higher current capabilities [13] - [16].

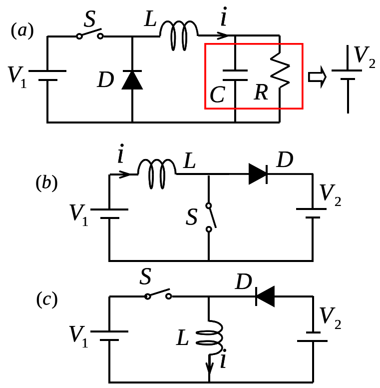

Figure 1: Basic PWC models. (a) Buck converter (b) Boost converter (c) Buck-boost converter.

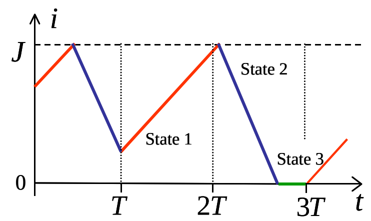

Figure 2: Switching rules

2. PWC Models of Basic DC/DC Converters

Fig. 1 (a) shows the basic buck converter. The switch S and diode D can be either of the following three states.

State 1: S conducting, D blocking and $0 < i < J$
State 2: S blocking, D conducting and $0 < i < J$
State 3: S and D both blocking and $i = 0$

As shown in Fig. 2, the inductor current i increases to a threshold J in State 1, decreases to zero in State 2 and does not change in State 3. The transition between these three states is defined by the switching rule depending on the inductor current i and a clock signal with period T: State 1 is changed into State 2 if $i = J$ (even if $t = nT$), State 2 is changed into State 1 if $t = nT$, State 2 is changed into State 3 if i reaches 0 (even if $t = nT$), and State 3 is changed into State 1 if $t = nT$, where n is a nonnegative integer. If the system operates to (not to) include State 3 then the system is said to operate in a discontinuous conduction mode (ab.

DCM) (continuous conduction mode (ab. CCM)). In order to simplify the analysis, we assume that the time constant RC is much greater than the period T. In this case the load can be replaced with a constant voltage source V_2 [10] and the circuit dynamics can be simplified into Eq. (1).

$$L\frac{d}{dt}i = \begin{cases} V_1 - V_2 & \text{for State 1} \\ -V_2 & \text{for State 2} \\ 0 & \text{for State 3} \end{cases}, \quad 0 < V_2 < V_1, \qquad (1)$$

where all the circuit elements are assumed to be ideal. This is the PWC model having piecewise linear solutions. Using the dimensionless variables and parameters,

$$\tau = \frac{t}{T},\ x = \frac{i}{J},\ a = \frac{T}{LJ}(V_1 - V_2),\ b = \frac{T}{LJ}V_2, \qquad (2)$$

Eq. (1) and the switching rule are transformed into

$$\frac{d}{d\tau}x = \begin{cases} a & \text{for State 1} \\ -b & \text{for State 2} \\ 0 & \text{for State 3} \end{cases} \qquad (3)$$

State 1 $\rightarrow$ State 2 if $x = 1$
State 2 $\rightarrow$ State 1 if $\tau = n$.
State 2 $\rightarrow$ State 3 if $x = 0$
State 3 $\rightarrow$ State 1 if $\tau = n$

In a likewise manner we can derive the PWC models of boost and buck-boost converters as shown in Fig. 1 (b) and (c), respectively. The switching rules of these models are the same as the buck converter. The two PWC models can be transformed into Eq.(3) where $a = \frac{T}{LJ}V_1$ and $b = \frac{T}{LJ}(V_2 - V_1)$ for the boost converter and $a = \frac{T}{LJ}V_1$ and $b = \frac{T}{LJ}V_2$ for the buck-boost converter. Note that the original five parameters (T, L, J, V_1, V_2) of the PWC models are integrated into the dimensionless two positive parameters $a > 0$ and $b > 0$ of Eq.(3).

3. Piecewise Linear Return Map

Here we derive return map from Eq. (3) and clarify the basic dynamics. Let $x_n \equiv x(n)$ and let $I \equiv [0, 1]$. Since $x_{n+1} \in I$ is determined by $x_n \in I$, we can define the return map f and the dynamics can be reduced into the iteration:

$$x_{n+1} = f(x_n), \quad f : I \rightarrow I. \qquad (4)$$

For the return map we define basic periodic phenomena. A pint $x_p \in I$ is said to be a periodic point with period k if $f^k(x_p) = x_p$ and $f^l(x_p) \neq x_p$ for $1 \leq l < k$ (l is meaningless for $k = 1$), where f^k is the k-fold composition of f. A periodic point with period 1 is referred to as a fixed point. A sequence of periodic points with period k, $\{f(x_p), \cdots, f^k x_p\}$ is said to be a periodic orbit with period k. The periodic orbit is said to be stable (respectively, superstable) if $|Df^k(x_p)| < 1$ (respectively, $Df^k(x_p) = 0$) where $Df^k(x_p)$ is the slope of f^k at x_p. A stable periodic

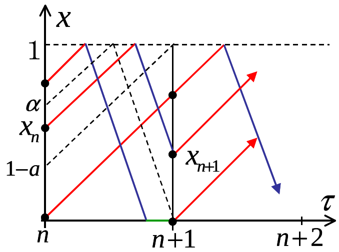

Figure 3: Basic orbits for $(a, b) \in D_a$.

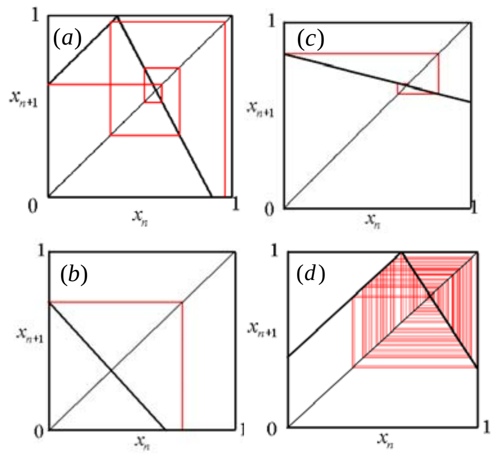

Figure 4: Typical return maps. (a) (a^{-1}, b^{-1})=(1.61, 0.82) $\in D_a$, (b) (a^{-1}, b^{-1})=(0.6, 2.3) $\in D_b$, (c) (a^{-1}, b^{-1})=(0.8, 0.7) $\in D_c$, (d) (a^{-1}, b^{-1})=(2.5, 1.5) $\in D_d$.

orbit corresponds to a stable periodic waveform in CCM. A superstable periodic orbit with period k (ab. k-SPO)

corresponds to superstable periodic waveform with period kT in DCM. If $|Df^q(x)| > 1$ is satisfied for almost all $x \in I$ and some finite integer q, the map f is ergodic and has one positive Lyapunov exponent [11]. In this case f is said to exhibit chaos: it corresponds to chaotic waveform in CCM. Since the shape of the map depends on the parameters, we introduce five subspaces of the parameters.

$$\begin{aligned} D_a &\equiv \{(a, b) |\ a^{-1} > 1 > b^{-1}\} \\ D_b &\equiv \{(a, b) |\ a^{-1} + b^{-1} > 1,\ a^{-1} < 1,\ b^{-1} < 1\} \\ D_c &\equiv \{(a, b) |\ a^{-1} + b^{-1} > 1,\ a^{-1} < 1 < b^{-1}\} \\ D_d &\equiv \{(a, b) |\ a^{-1} > 1,\ b^{-1} > 1\} \\ D_e &\equiv \{(a, b) |\ a^{-1} + b^{-1} < 1\} \end{aligned} \qquad (5)$$

In each subspace return map can be described as a piecewise linear function and basic dynamics can be clarified. Fig. 3 illustrates the dynamics for $(a, b) \in D_a$. The system is in State 1 at $\tau = n$ and the orbits for $n \leq \tau < n + 1$ are classified into three cases: (i) x increases without reaching the threshold $x = 1$, (ii) x reaches $x = 1$ and decreases without $x = 0$, and (iii) x reaches $x = 1$, decreases, and reaches $x = 0$. The return map consists of three segments

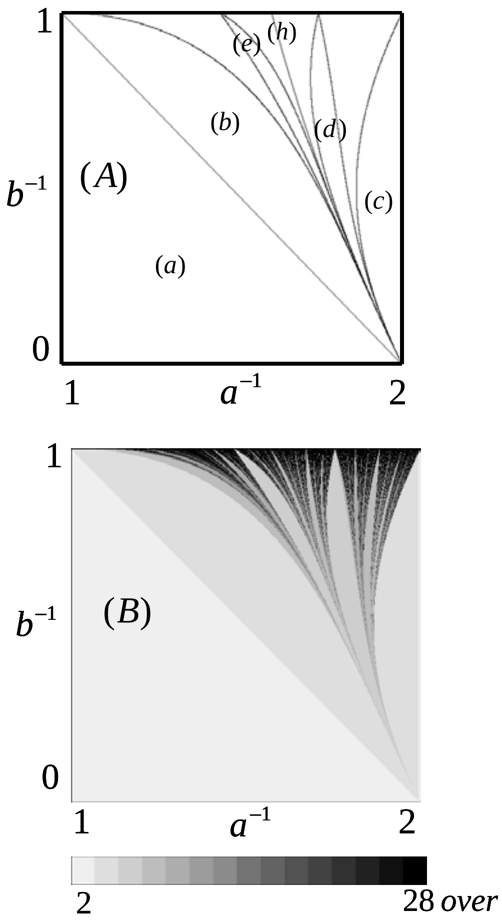

Figure 5: Diagram of SPOs. In (B) the tone is to be dark as the period of SPO increases.

corresponding to the three cases:

$$f(x_n) = \begin{cases} x_n + a & \text{for } 0 \le x_n < 1 - a \\ -px_n + \beta & \text{for } 1 - a \le x_n < \alpha \\ 0 & \text{for } \alpha \le x_n \le 1 \end{cases} \qquad (6)$$

$$\alpha \equiv 1 - a(1 - b^{-1}), \quad \beta \equiv 1 - b(1 - a^{-1}), \quad p \equiv ba^{-1}.$$

This return map has unique SPO with period 2 or more. As shown in Fig. 4 (a) this map has flat part and the SPO must pass through 0: the period can be counted easily in numerical simulation. For $1 < a^{-1} < 2$ and $0 \le b^{-1} \le 1$ existence regions of some SPOs can be identified as (a) to (e) in Fig. 5 (A):

$$\begin{aligned} &\text{(a) 2-SPO:} && \beta \le g_1(a,b) \equiv p\left(-\frac{\beta}{p} + \frac{1}{p} + 1\right) \\ &\text{(b) 4-SPO:} && g_1(a,b) < \beta \le g_2(a,b) \\ &\text{(c) 3-SPO:} && \beta < g_3(a,b) \equiv \frac{-p^2}{-p+1}\left(-\frac{\beta}{p} + \frac{1}{p} + 1\right) \\ &\text{(d) 5-SPO:} && g_4(a,b) \le \beta \le g_5(a,b) \\ &\text{(e) 6-SPO:} && g_6(a,b) \le \beta \le g_7(a,b) \end{aligned} \qquad (7)$$

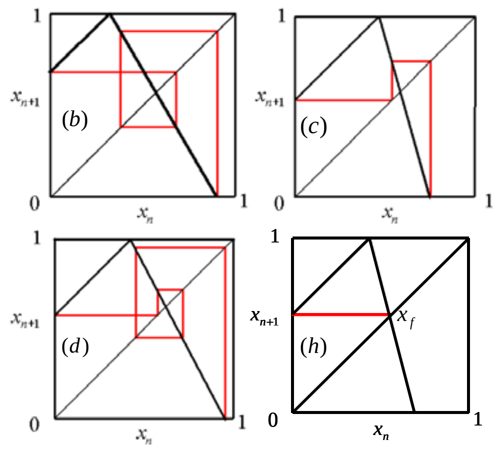

Figure 6: Typical orbits. (b) 4-SPO for $(a^{-1}, b^{-1}) = (1.48, 0.838)$, (c) 3-SPO for $(a^{-1}, b^{-1}) = (1.87, 0.512)$, (d) 5-SPO for $(a^{-1}, b^{-1}) = (1.738, 0.91)$, (h) Unstable fixed point for $(a^{-1}, b^{-1}) = (1.8, 0.45)$

where

$$\begin{aligned} g_2(a,b) &\equiv \frac{p^3}{p^2 - p + 1}\left(-\frac{\beta}{p} + \frac{1}{p} + 1\right) \\ g_4(a,b) &\equiv \frac{-p^4}{-p^3 + p^2 - p + 1}\left(-\frac{\beta}{p} + \frac{1}{p} + 1\right) \\ g_5(a,b) &\equiv \frac{p^3 + p}{p^2 - p + 1}\left(-\frac{\beta}{p} + \frac{1}{p} + 1\right) \\ g_6(a,b) &\equiv \frac{-p^4 + p}{-p^3 + p^2 - p + 1}\left(-\frac{\beta}{p} + \frac{1}{p} + 1\right) \\ g_7(a,b) &\equiv \frac{p^5}{p^4 - p^3 + p^2 - p + 1}\left(-\frac{\beta}{p} + \frac{1}{p} + 1\right) \end{aligned}$$

Except for these regions the map has rich SPOs as shown in Fig. 5 (B). Special attention should be paid for the curve (h): the map has an unstable fixed point $x_f = (1+p)\left(-\frac{\beta}{p} + \frac{1}{p} + 1\right)$ and $f(0) = x_f$ is satisfied. Near this many complicated SPOs can be observed. We then describe return maps in subspaces D_b to D_e. Fig. 4 illustrates typical shapes of the maps.

Return map for $(a,b) \in D_b$ is given by Eq. (8).

$$f(x_n) = \begin{cases} -px_n + \beta & \text{for } 0 \le x_n < \alpha \\ 0 & \text{for } \alpha \le x_n \le 1 \end{cases} \qquad (8)$$

If $p < 1$ the map has a stable fixed point. If $p > 1$ the map has a SPO with period 2.

Return map for $(a,b) \in D_c$ is given by Eq. (9): the map has a stable fixed point as shown in Fig. 4 (c).

$$f(x_n) = -px_n + \beta, \quad \text{for } 0 \le x_n \le 1. \qquad (9)$$

Return map for $(a,b) \in D_d$ is given by Eq. (10).

$$f(x_n) = \begin{cases} x_n + a & \text{for } 0 \le x_n < 1 - a \\ -px_n + \beta & \text{for } 1 - a \le x_n < 1 \end{cases} \qquad (10)$$

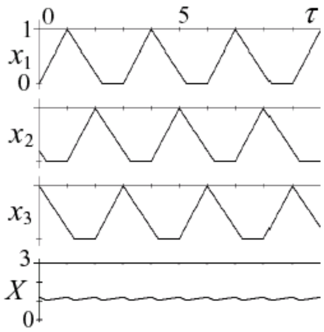

Figure 7: 3-phase synchronization in DCM for $(a, b) = (1.00, 0.80)$. $X \equiv x_1 + x_2 + x_3$.

If $p < 1$ the map has a stable fixed point. If $p > 1$ the map exhibits chaos as discussed in [17].

Return map for $(a, b) \in D_e$ is given by Eq. (11): the map has a superstable fixed point $x_f = 0$.

$$f(x_n) = 0 \quad \text{for } 0 \le x_n \le 1. \tag{11}$$

4. Application to Interleaved Buck Converters

Since the superstable periodic waveform in DCM has vary fast transient process, it may be useful in the interleaved buck converters (ab. IBC [13]). The IBC is constructed by interleaving N identical buck converters between voltage source V_1 and the load. The PWC model is described by Equation (12).

$$\frac{d}{d\tau}x_i = \begin{cases} a & \text{for State 1} \\ -b & \text{for State 2} \\ 0 & \text{for State 3} \end{cases} \quad i \in \{1, \cdots, N\}, \tag{12}$$

State 1 → State 2 if $x_i = 1$
State 2 → State 1 if $x_i =$ the minimum at $\tau = n$.
State 2 → State 3 if $x_i = 0$
State 3 → State 1 if $\tau = n$

where x_i is proportional to the inductor current of i-th converter and (a, b) is given by Equation (2). Note that the connection is realized by the switchings to State 1. Fig. 7 shows typical waveforms where $X \equiv x_1 + x_2 + x_3$ is proportional to the output current by the current sharing. In this case ripple reduction is possible with vary fast transient process. We can guarantee that the IBC exhibits N-phase synchronization in DCM if

$$N - 1 < a^{-1} + b^{-1} < N, \quad \text{or equivalently}$$
$$\frac{LJV_1}{NV_2(V_1 - V_2)} < T < \frac{LJV_1}{(N-1)V_2(V_1 - V_2)}. \tag{13}$$

It should be noted that adjusting T can realize this N-phase synchronization for any values of V_1 and V_2.

5. Conclusions

The PWC models of basic DC/DC converters is discussed. Using the piecewise linear return map, basic periodic and chaotic phenomena are clarified in terms of the two essential parameters. In the DCM, we have analyzed some of interesting SPOs. Application to efficient interleaved converters is also introduced. Future problems include analysis of SPOs in DCM and implementation of practical circuits.

References

[1] C. K. Tse and M. di Bernardo, Complex behavior in switching power converters, Proc. IEEE, 90, pp. 768-781, 2002.

[2] J.H.B. Deane, Chaos in a current-mode controlled boost dc-dc converter, IEEE Trans. Circuits Systs. I, 39, pp.680-683, 1992.

[3] C. K. Tse, Flip bifurcation and chaos in three-state boost switching regulators, IEEE Trans. Circuits Systs. I, 41, pp. 16-23, 1994.

[4] S. Banerjee, M. S. Karthik, G. Yuan and J. A. Yorke, Bifurcation in one-dimensional piecewise smooth maps - theory and applications in switching circuits, IEEE Trans. Circuits Systs. I, 47, pp. 389-394, 2000.

[5] H. H. C. Iu and C. K. Tse, Bifurcation behavior in parallel-connected buck converters, IEEE Trans. Circuits Systs. I, 48, pp.233-240, 2001.

[6] S. Parui and S. Banerjee, Bifurcations due to transition from continuous conduction mode to discontinuous conduction mode in the boost converter, IEEE Trans. Circuits Systs. I, 50, pp. 1464-1469, 2003.

[7] J. H. B. Deane and D. C. Hamill, Improvement of power supply EMC by chaos, Electron. Lett. 32, 12, p. 1045, 1996

[8] Y. H. Lim and D. C. Hamill, Chaos in spacecraft power systems, Electron. Lett. 35, 9, pp. 510-511, 1999.

[9] D. C. Hamill and D. J. Jeffries, Subharmonics and chaos in a controlled switched-mode power converter, IEEE Trans. Circuits Systs. I, 35, pp. 1059-1061, 1988.

[10] J. H. B. Deane, P. Ashwin, D. C. Hamill and D. J. Jeffries, Calculation of the periodic spectral components in a chaotic DC-DC converter, IEEE Trans. Circuits Systs. I, 46, pp.1313-1319, 1999.

[11] T. Saito, H. Torikai and W. Schwarz, Switched dynamical systems with double periodic inputs: an analysis tool and its application to the buck-boost converter, IEEE Trans. Circuits Systs. I, 47, pp.1038-1046, 2000.

[12] S. Tasaki and T. Saito, Analysis of parallel connected buck converters with WTA, Technical Report of the IEICE, NLP2002-143, 2003.

[13] T. Saito, S. Tasaki and H. Torikai, WTA-based interleaved buck converters for low-voltage high-current applications, Proc. IEEE/IECON, pp. 640-643, 2003.

[14] R. Giral and L. Murtinez-Salamero, Interleaved converters operation based on CMC, IEEE Trans. Power Electron., 14, 4, pp.643-652, 1999

[15] X. Zhou, P. Xu and F. C. Lee, A novel current-sharing control technique for low-voltage high-current voltage regulator module applications, IEEE Trans. Power Electron., 15, 6, pp.1153-1162, 2000.

[16] S. K. Mazumder, A. H. Nayfeh and D. Borojevic, Robust control of parallel DC-DC buck converters by combining integral-variable-structure and multiple-sliding-surface control schemes, IEEE Trans. Power Electron., 17, pp.428-437, 2002.

[17] S. Ito, S. Tanaka and H. Nakada, On unimodal linear transformations and chaos II, Tokyo J. Math., 2, 2, pp. 241-259, 1979.